Influence of Gaseous Environments on Rates of Near-Threshold Fatigue Crack Propagation in NiCrMoV Steel

PETER K. LIAW, S. J. HUDAK, Jr., and J. KEITH DONALD

The influence of hydrogen environment (448 kPa) on near-threshold fatigue crack propagation rates was examined in a 779 MPa yield strength NiCrMoV steel at 93 °C. An automatically decreasing and increasing stress intensity technique was employed to generate crack growth rates at three load ratios (R = 0.1, 0.5, and 0.8). Results show that the crack propagation rates in hydrogen are slower than those in air for levels of stress intensity range, ΔK, below about 12 MPa$\sqrt{m}$. The crack closure concept does not explain the slower crack growth rates in hydrogen than in air. Near-threshold growth rates appear to be controlled by the levels of residual moisture in the environments. In argon and air, the fracture morphology is transgranular, while in H_2 the amount of intergranularity varies with ΔK and achieves a maximum when the cyclic plastic zone is approximately equal to the prior austenite grain size.

I. INTRODUCTION

MOST of the available fatigue crack propagation rate data have been generated in the Paris region; consequently, relatively little data are available on near-threshold crack propagation. However, many machine components are often subject to a low-stress and high-cycle fatigue condition, and data regarding the rates of near-threshold crack growth are of vital importance to assure the successful application of a fracture mechanics methodology in fatigue life prediction. Information in this region is also important is formulating a broader view of the mechanisms of fatigue crack growth—particularly for those aspects involving microstructural and environmental effects.

The rate of near-threshold fatigue crack growth is more affected by mean stress, microstructure, and environment than crack propagation in the Paris region.[1-10] It has been reported that load ratios ($R = \sigma_{min}/\sigma_{max}$) influence the near-threshold crack growth rate, da/dN, with increased R being accompanied by an increase in da/dN.[1,2] Grain size strongly affected the near-threshold crack growth behavior in steels, titanium, and aluminum alloys,[2-10] while the crack growth rates in the Paris region were hardly influenced. In reference to the effects of environments on the rates of threshold crack growth, there is little understanding and contradictory results exist. Even though corrosive environments increase the Paris-region fatigue crack growth rates, it is not necessarily true in the near-threshold region. Previous results[1,11] revealed that a water environment indeed lessened, or had no effect on, threshold crack propagation rates in steels, as compared to ambient air. Nevertheless, with the elimination of the corrosive environments, near-threshold crack propagation resistance was increased in vacuum for steels and aluminum alloys.[5-7,12-14] Further experiments are necessary to understand the behavior of near-threshold crack growth in corrosive environments.

In general, hydrogen environments increase the rates of Paris-region fatigue crack propagation in steels. It has been proposed that hydrogen embrittlement is the reason for promoting crack growth. However, relatively limited work on near-threshold crack growth behavior has been carried out in hydrogen environments.[15-21] In this investigation, near-threshold fatigue crack propagation experiments were conducted at 93 °C with an NiCrMoV steel exposed to hydrogen, air, or argon. Crack growth rate data at various load ratios were generated by using an automatically decreasing ΔK technique. Possible mechanisms for the influence of hydrogen on the rates of near-threshold crack propagation are discussed. Previous crack growth rate results developed for a NiMoV steel[15] were used for comparison with the present NiCrMoV steel.

II. MATERIAL

All near-threshold fatigue crack growth rate testing was conducted with a 779 MPa yield strength NiCrMoV rotor steel (similar to ASTM A471) supplied as sections cut from a large forging. The chemical composition of the steel in wt pct is: 0.24C, 0.28Mn, 3.51Ni, 0.005P, 0.04S, 0.012Si, 1.64Cr, 0.11V, 0.39Mo, and balance Fe. The material was austenitized at 843 °C and subsequently quenched and tempered at approximately 590 °C for 40 hours. The mechanical properties are listed in Table I. This steel has a bainite microstructure with a prior austenite grain size ranging from 10 to 43 μm.

III. TEST METHOD

A WOL (wedge-open-loading) type compact toughness specimen, 64.8 mm wide (W), 63 mm high, and 6.4 mm thick, was utilized to generate the threshold fatigue crack growth rate data. Prior to testing, the specimens were

Table I. Mechanical Properties of Ni-Cr-Mo-V Steel*

0.2 Pct Yield Strength (MPa)		Ultimate Tensile Strength (MPa)	Reduction in Area (Pct)
24 °C	93 °C	24 °C	24 °C
779	737	882	63

*From References 22 to 24

PETER K. LIAW is Senior Engineer with Westinghouse Research and Development Center, Materials Engineering Department. S. J. HUDAK, Jr. is Senior Scientist with Southwest Research Institute, Materials Sciences Department. J. KEITH DONALD is Vice President, Del Research Division of Professional Services Group Incorporated.

Manuscript submitted November 25, 1981.

ISSN 0360-2133/82/0911-1633$00.75/0

precracked about 2.3 mm beyond the initial machined notch in accordance with ASTM Standard E647.[25] The crack propagation test was performed on an MTS closed loop, electrohydraulic fatigue machine using a sinusoidal waveform at a frequency of 120 Hz.

The environments investigated were: (a) 448 kPa hydrogen gas (99.95 pct purity), (b) ambient air (relative humidity $\approx$ 30 to 40 pct, and (c) 448 kPa argon gas ($\sim$ 99.95 pct purity). The hydrogen and argon gases (continuous flow) were contained in a stainless steel, O-ring sealed chamber clamped to each side of the specimen. Prior to the start of each test, hydrogen, or argon gas was flushed through the chamber to remove residual impurities. Based on the purity of the bottle gas and the experimental procedure, the moisture contents in hydrogen and argon are estimated to be less than 10 ppm. The specimens were heated to a testing temperature of 93 °C by using resistive heating tapes. A thermocouple installed in the proximity of the crack was used to monitor the temperature.

The near-threshold fatigue crack growth rate data were developed by using an automated technique. The MTS fatigue machine was interfaced with a PDP-8-e computer. The crack length was monitored utilizing the compliance technique. The computerized system allows the stress intensity range, ΔK, to be continuously decreased (or increased) in accordance with the following equation, as proposed by Saxena, *et al*,[26]

$$\Delta K = \Delta K_0 \exp [c(a - a_0)] \qquad [1]$$

where a is the crack length, ΔK_0 and a_0 are the beginning stress intensity range and crack length, respectively, and c is a constant having a unit of reciprocal length.

Equation [1] provides a constant rate of change of plastic zone size, thereby eliminating effects of test history which may occur, for example, if step decreases in load are employed.[26] The c parameter controls the rate of decrease (or increase) in the plastic zone size with respect to crack length. The values of c used in this investigation are $\pm$ 0.098 mm^{-1} which corresponds to a ΔK change of about 5 pct for crack extension of 0.5 mm. In each specimen, a decreasing ΔK ($c = -0.098$ mm^{-1}) test was carried out to develop the rates of near-threshold crack growth, and an increasing ΔK test ($c = +0.098$ mm^{-1}) was then performed to acquire higher crack propagation rates. The expression used to compute stress intensity range for the WOL specimen can be found in Reference 27.

The fatigue crack growth rate was calculated by a secant method in which the crack length increment bridges the adjacent first and third *a vs N* (loading cycle) data with ΔK corresponding to the midpoint in the increment. The threshold stress intensity range, ΔK_{th}, is operationally defined as the stress intensity range corresponding to a crack growth rate of 1.0×10^{-7} mm per cycle. This is accomplished by fitting a least-squares line for the propagation rates ranging from 5×10^{-7} to 5×10^{-8} mm per cycle, and ΔK_{th} is determined at 1.0×10^{-7} mm per cycle.

IV. EXPERIMENTAL RESULTS

A. *Influence of R Values and Gaseous Environments*

The rates of near-threshold crack propagation at three R values are provided in Figures 1(a) and 1(b) for air and hydrogen environments, respectively. The effect of R on fatigue crack growth rates becomes more pronounced as the crack growth rate decreases. Increasing R values increases the near-threshold crack propagation rates in both air and

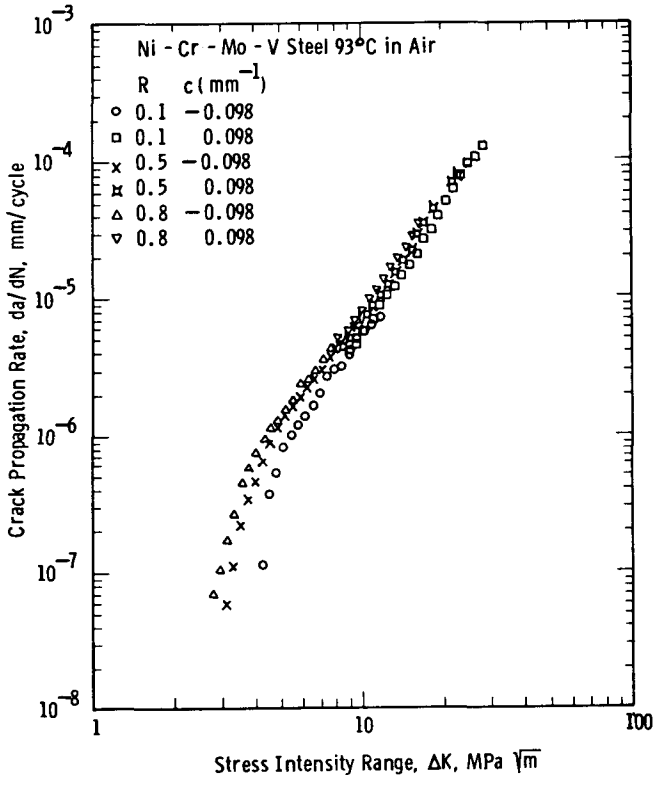

Fig. 1 — (*a*) The effect of R-ratio on crack growth rates in NiCrMoV steel in air at 93 °C. (*b*) The effect of R-ratio on crack growth rates in NiCrMoV steel in 448 kPa H_2 at 93 °C.

hydrogen for the NiCrMoV steel. The same results have been noted earlier in other steels.[1,2,11,14,15,26,29]

The crack growth rate data at 93 °C in hydrogen and air are compared in Figures 2(a) to 2(c). For all three R values, the 448 kPa hydrogen gas decreases the near-threshold crack propagation rate relative to that of ambient air. These results are consistent with those in two relatively high-strength NiMoV and 300 M steels[15,16,17] with yield strength of 660 and 1700 MPa$\sqrt{m}$, respectively. Nevertheless, as the value of ΔK exceeds approximately 12 MPa$\sqrt{m}$ in Figures 2(a) through 2(c), the fatigue crack growth rates in hydrogen are accelerated and eventually become faster than those in air. Similar results in this growth rate regime have previously been observed in an NiMoV steel.[18,22]

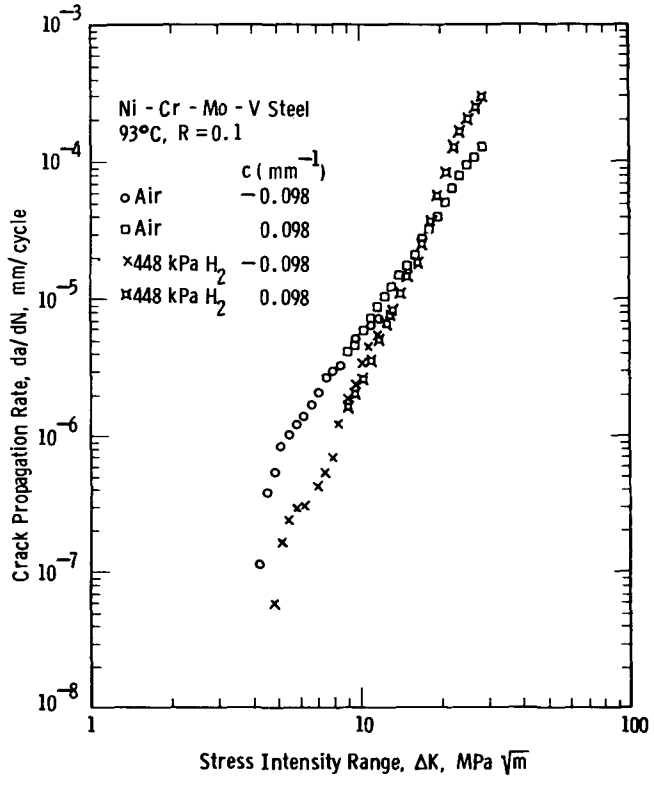

(a)

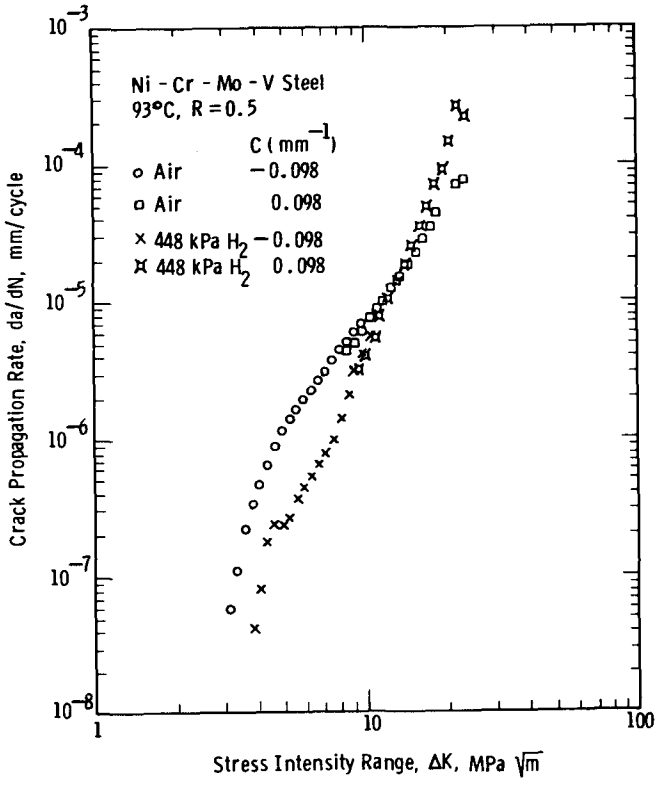

(b)

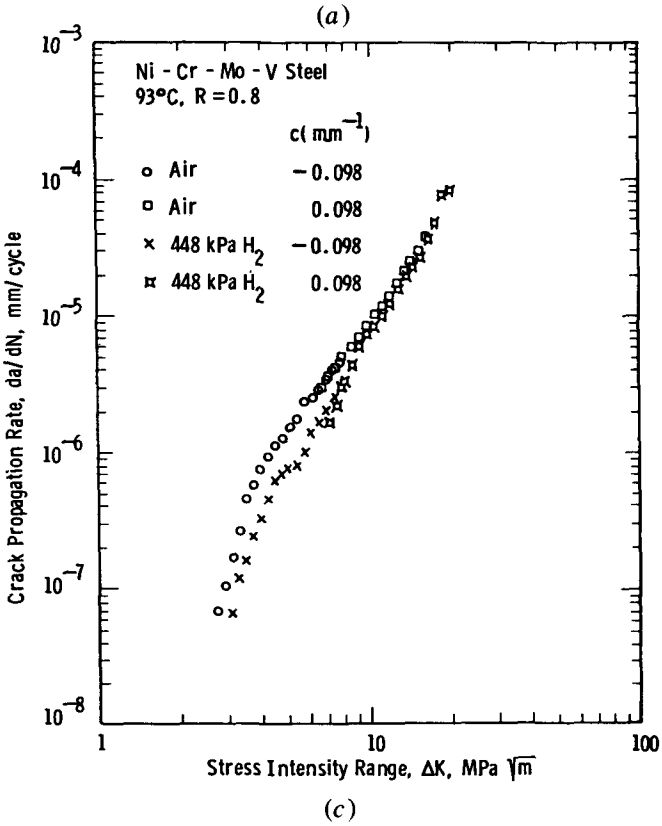

(c)

Fig. 2—(*a*) The effect of environment on crack growth rates in NiCrMoV steel at 93 °C and R = 0.1. (*b*) The effect of environment on crack growth rates in NiCrMoV steel at 93 °C and R = 0.5.(*c*) The effect of environment on crack growth rates in NiCrMoV steel at 93 °C and R = 0.8.

Figure 3 illustrates the combined effects of hydrogen and R values on ΔK_{th} at 93 °C in the NiCrMoV steel. When R values decrease, the values of ΔK_{th} increase in both hydrogen and air environments. In the 448 kPa H_2 atmosphere, ΔK_{th} is larger than that in air regardless of load ratios. Interestingly, in air and at $R = 0.1$, the present value of ΔK_{th} is smaller than that of 7.0 MPa$\sqrt{m}$ in a 575 MPa yield strength NiCrMoV steel tested at 23 °C.[20]

Figure 4 demonstrates that at low ΔK values less than about 12 MPa$\sqrt{m}$, the near-threshold crack propagation rates in argon are comparable to those in hydrogen. Similar results were noted in 2.25Cr-1Mo steels,[17] *i.e.*, the rates of threshold crack growth in hydrogen and helium are nearly the same. At ΔK levels larger than approximately 12 MPa$\sqrt{m}$, the growth rates in hydrogen become increasingly faster than those in argon (Figure 4). A comparison of threshold crack propagation behavior in air and argon is also shown in Figure 4. The rates of crack propagation in argon are slower than those in air over the entire range of ΔK examined.

B. *Fracture Morphology*

The fracture morphology is transgranular at the threshold irrespective of R ratios and environments. As shown in Figures 5(a) to 5(c), there is little difference among fracture surfaces at the threshold in hydrogen, air, and argon environments. The morphology of the fatigue crack growth surfaces in air and argon exhibits typical transgranular features for the entire range of ΔK studied (Figures 5(a) and 5(c)). In hydrogen gas, transgranular fracture was found at the threshold ΔK levels. However, when the value of ΔK increases, intergranular fracture starts to appear, approaches a maximum, and then decreases to completely transgranular cracking (Figure 5(b)), as reported in other steels.[15,19,20] In Figures 5(a) to 5(c), secondary cracking tends to increase with an increase in ΔK.

The relationship between ΔK and intergranular fracture observed in the 448 kPa hydrogen atmosphere is shown in Figure 6. Interestingly, the largest percentage of intergranularity takes place at $\Delta K = 11.3$ MPa$\sqrt{m}$, regardless of the R value. Increasing the R ratio reduces the percentage of intergranularity at a given value of ΔK. Similar findings were also reported in other steels.[14,15,21] Note that in Figure 6, the maximum intergranularity occurs at a ΔK value of 11.3 MPa$\sqrt{m}$, which is close to that (~12 MPa$\sqrt{m}$) for the transition from where the crack growth rates in H_2 begin to exceed those in air (Figures 2(a) and 2(b)).

C. *Determination of Oxide Thickness at the Threshold*

Auger analyses were performed to determine the thickness of oxides on the fracture surfaces in air, hydrogen, and argon environments at $R = 0.5$. The sputtering rate in the Auger spectrometer was calibrated using profilometry on steel surfaces after sputtering. The results are illustrated in Figure 7 which plots the at. pcts of iron and oxygen *vs* the average distance from the free surface into the oxide, d. The thickness of the oxide is defined as the value of d at which the iron and oxygen curves intersect.[30] The electron beam was scanned at TV-rates during the Auger analysis, and the area covered on the specimen for the analysis was a square of 400 μm^2. Therefore, the measured oxide thickness represents an average thickness in the threshold area. It is interesting to find that the thickness of the threshold oxide layer in hydrogen and argon environments is about the same

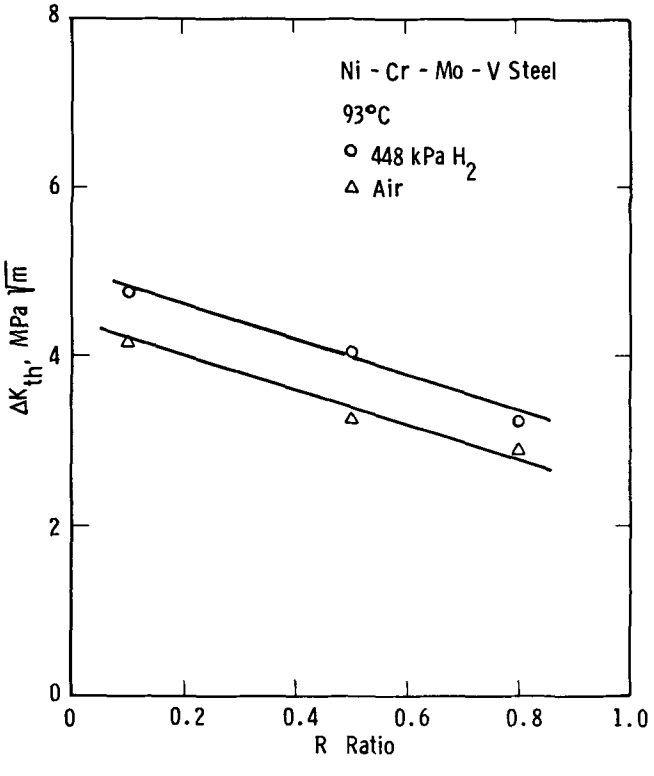

Fig. 3—Comparison of ΔK_{th} in hydrogen and air environments (NiCrMoV steel).

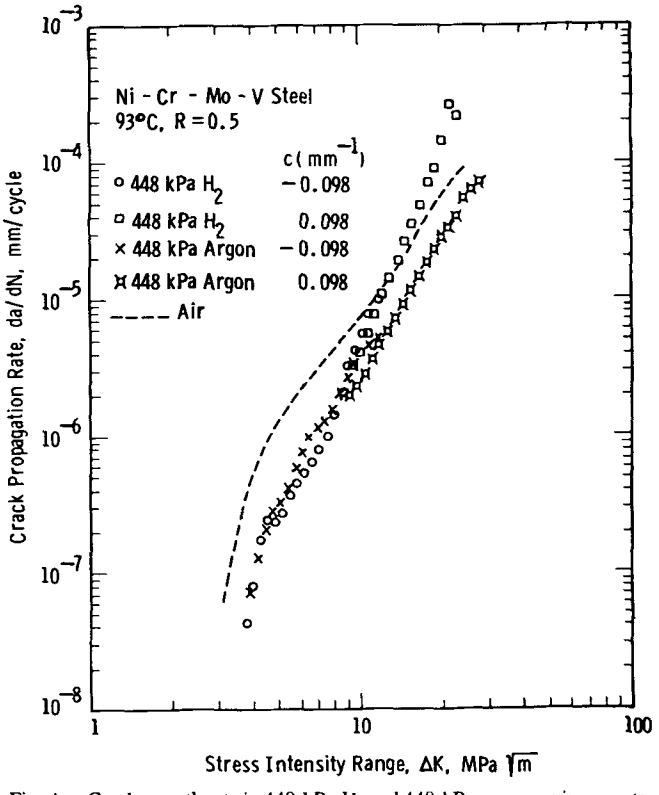

Fig. 4—Crack growth rate in 448 kPa H_2 and 448 kPa argon environments (NiCrMoV steel).

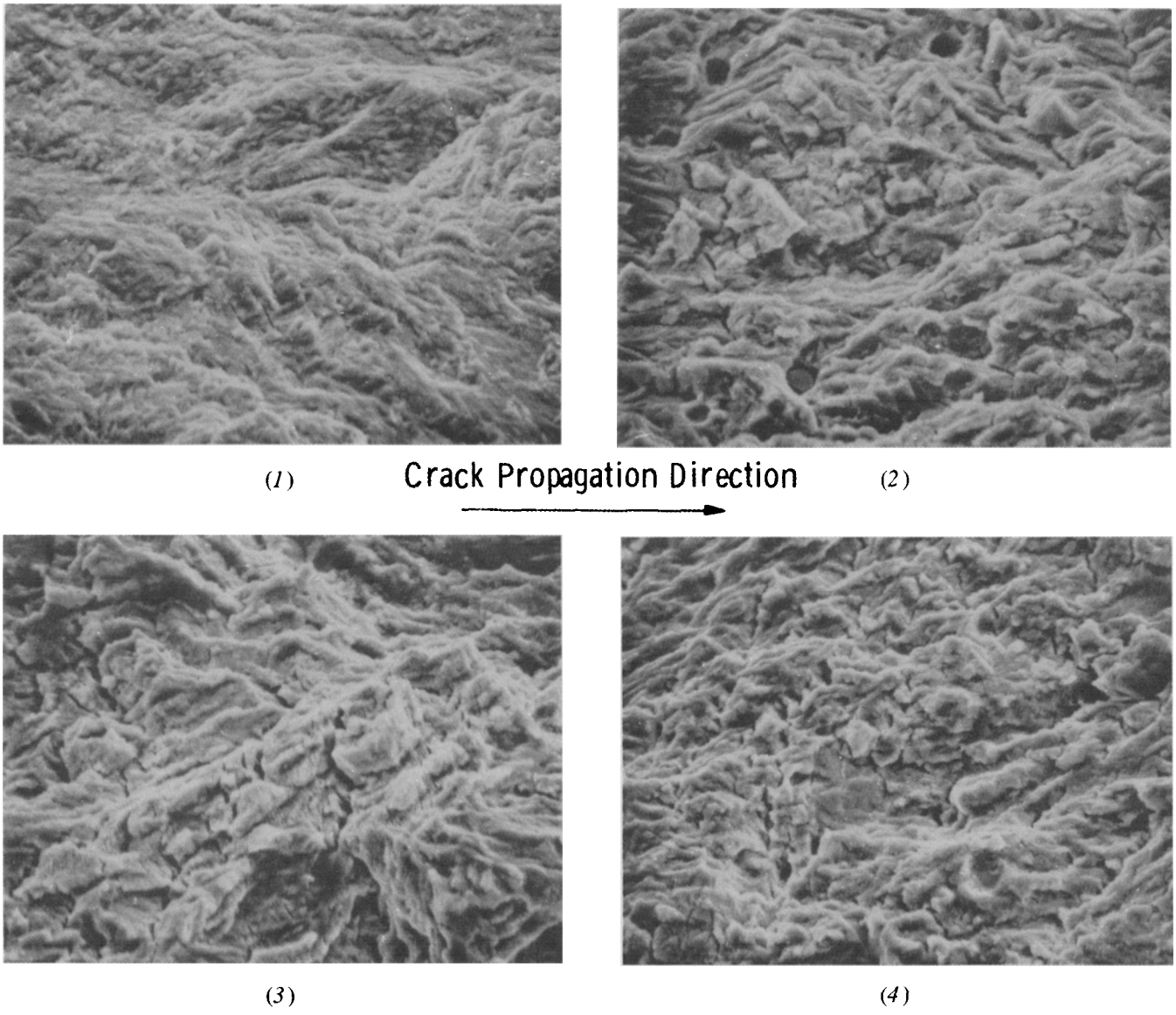

Fig. 5—(*a*) Fracture morphology in NiCrMoV steel at $R = 0.5$ in air (1) at the threshold, (2) $\Delta K = 8.9$ MPa$\sqrt{m}$, (3) $\Delta K = 13.4$ MPa$\sqrt{m}$, and (4) $\Delta K = 19.2$ MPa$\sqrt{m}$. Magnification 1770 times.

11Å, in Figure 7. However, the oxide thickness in air is about four times larger than that in hydrogen or argon.

V. DISCUSSION

A. *Effects of Gaseous Environments*

For the relatively higher strength NiCrMoV steel, 448 kPa hydrogen was found to decrease the crack propagation rates at the threshold levels (2 MPa$\sqrt{m} \lesssim \Delta K \lesssim$ 12 MPa$\sqrt{m}$) as compared to the ambient air behavior at 93 °C (Figures 2(a) to 2(c)). The data on near-threshold crack growth in the H_2 environment for this steel are not consistent with Ritchie's results for lower-strength 2.25Cr-1Mo steels with yield strength less than ~ 600 MPa.[16,17,19] At low R ratios (<0.5), the value of ΔK_{th} in 138 kPa hydrogen gas is smaller than that in the air environment for 2.25Cr-1Mo steels. However, at a high R value of 0.7, there are comparable threshold crack propagation rates in hydrogen and air. In high-strength 300 M steels[16,17] the near-threshold crack growth rates were found to be slower in hydrogen than in ambient air regardless of load ratios, which is in agreement with the present results. Thus, the influence of hydrogen on near-threshold crack propagation rates in steels appears to depend on strength level.[15,17] At low R values, lower-strength steels ($< \sim 600$ MPa) have lower ΔK_{th} values and faster crack growth rates in hydrogen gas, relative to ambient air, while in higher-strength steels the trend is reversed, regardless of R values.

Ritchie[16,17,19] successfully employed the crack closure concept to explain the increase of ΔK_{th} in ambient air relative to hydrogen for lower strength 2.25Cr-1Mo steels. In these studies, the near-threshold crack growth at low R ratios resulted in a thicker oxide layer in air than in hydrogen gas. Therefore, the oxide wedges the crack tip and increases

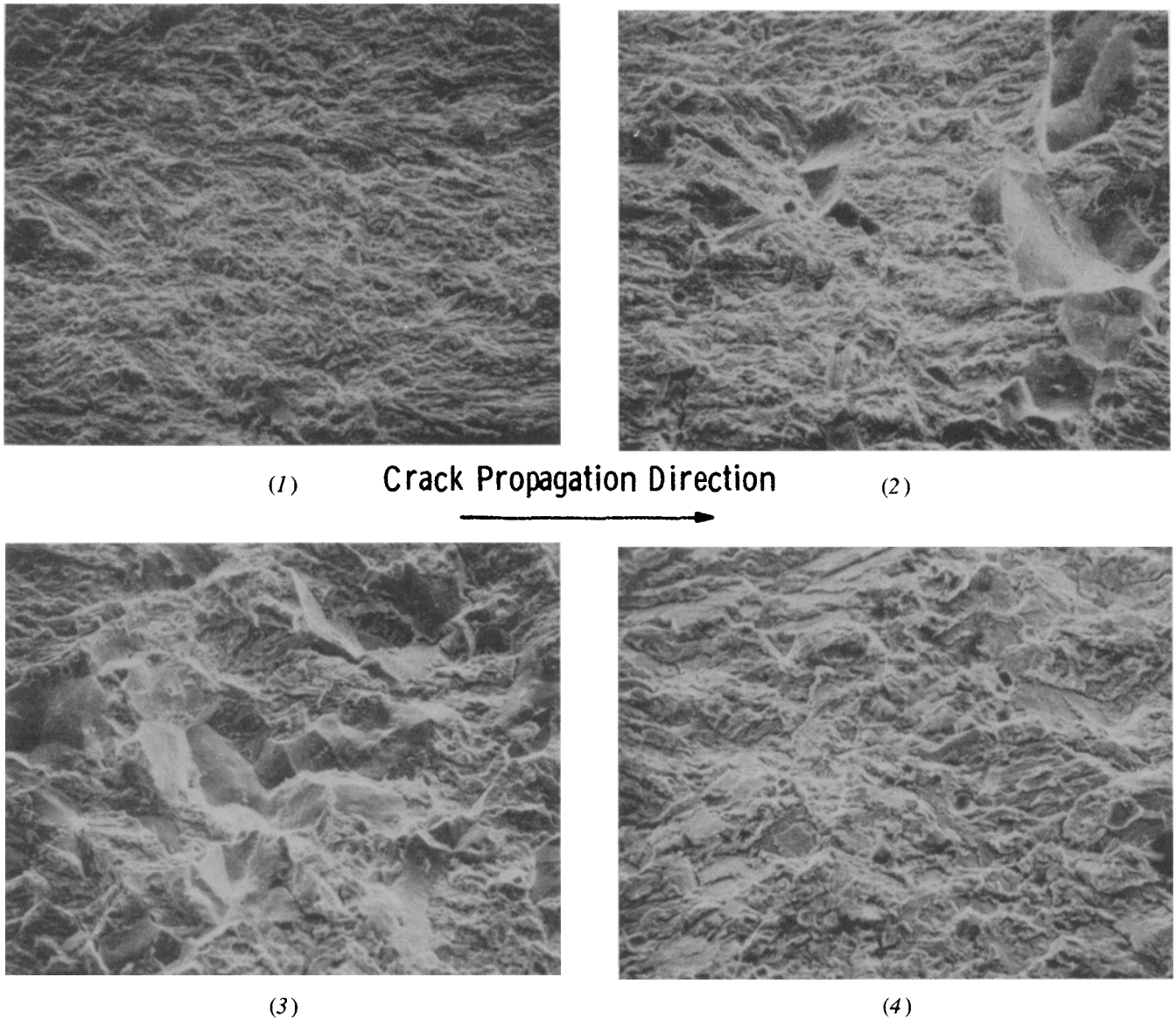

Fig. 5—(*b*) Fracture morphology in NiCrMoV steel at $R = 0.5$ in H_2 (1) at the threshold, (2) $\Delta K = 7.8$ MPa$\sqrt{m}$, (3) $\Delta K = 11.1$ MPa$\sqrt{m}$, and (4) $\Delta K = 20.1$ MPa$\sqrt{m}$. Magnification 440 times.

the closure level more significantly in air than in hydrogen. Consequently, the larger reduction in the effective stress intensity range ($\Delta K_{eff} = K_{max} - K_{closure}$) in air results in a decrease in the near-threshold crack propagation rates, compared to the hydrogen environment. As the value of R increases, the effect of oxide-induced crack closure on threshold crack growth is lessened. Consequently, at a high R ratio of 0.7, values of ΔK_{th} are comparable in air and hydrogen environments.[16,17,19]

In the present study, closure stress was measured by the unloading elastic compliance technique.[31] Using this technique, the unloading elastic displacement was subtracted from the total displacement to reveal the closure point.[31] In this investigation, crack closure was encountered only in tests with $R = 0.1$. The value of $\Delta K_{eff}/\Delta K$ decreases as the crack growth rate reaches the threshold in air and hydrogen environments (Figure 8(a)). That is to say, when the fatigue crack growth rate approaches the threshold level, the proportion of crack closure during each loading cycle increases. This is consistent with a theoretical model proposed by Purushothaman and Tien.[32] Similarly, McEvily[33] reported that as the fatigue crack moved toward the threshold region, crack closure might become more significant. In Figure 8(a), the crack closure stress intensity range ($= \Delta K - \Delta K_{eff}$) at the threshold occupies a large portion (approximately 30 pct) of ΔK. Thus, crack closure plays an important role in near-threshold crack growth behavior in this steel. The crack closure levels in air and hydrogen environments at a fixed value of ΔK are comparable in Figure 8(a) even though a slightly larger value of $\Delta K_{eff}/\Delta K$ was observed in air at low ΔK values. Hydrogen appears not to significantly affect the crack closure phenomenon in near-threshold crack propagation for NiCrMoV steel. As shown in the plot of da/dN *vs* ΔK_{eff} (Figure 8(b)), the difference

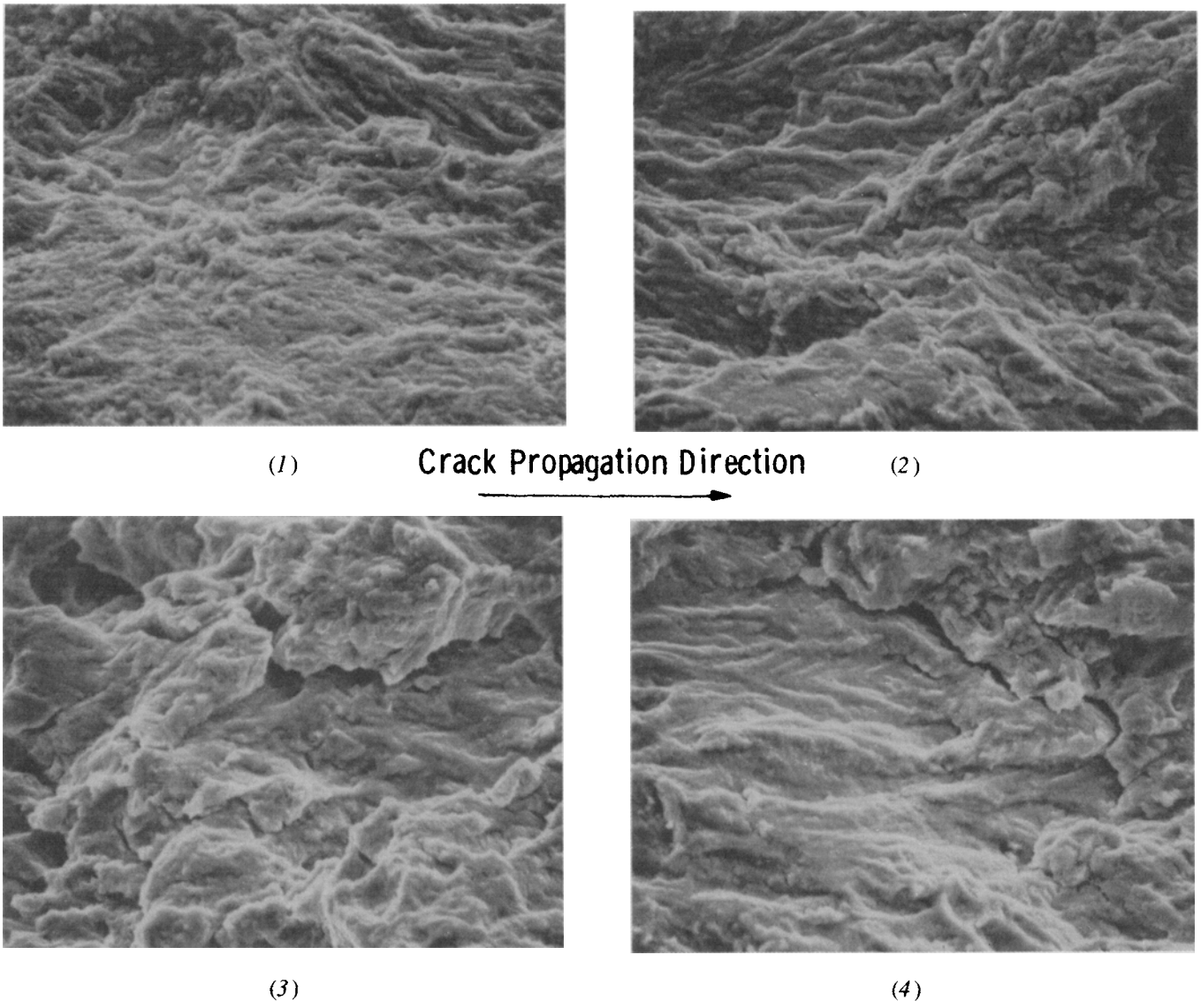

Fig. 5—(c) Fracture morphology in NiCrMoV steel at $R = 0.5$ in argon (1) at the threshold, (2) $\Delta K = 10.0$ MPa$\sqrt{m}$, (3) $\Delta K = 17.3$ MPa$\sqrt{m}$, and (4) $\Delta K = 25.5$ MPa$\sqrt{m}$. Magnification 1770 times.

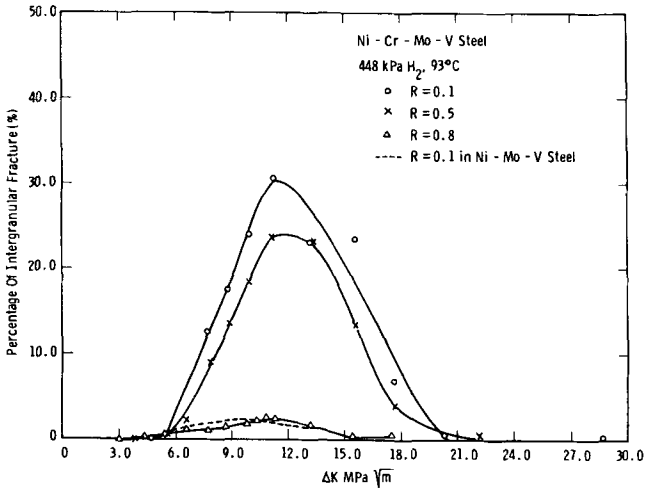

Fig. 6—The percentage of intergranularity *vs* ΔK in H_2 for NiCrMoV steel.

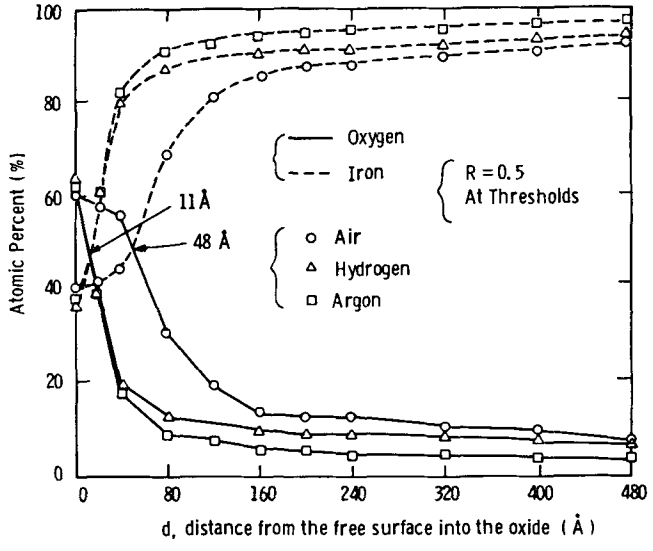

Fig. 7—Auger analysis of oxide at the threshold.

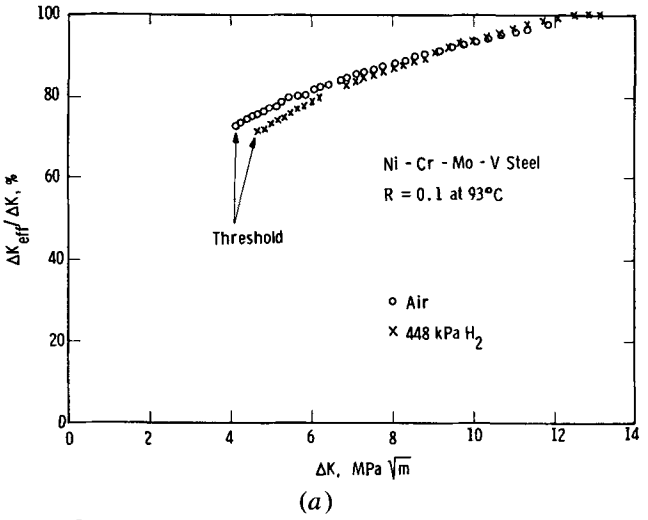

(a)

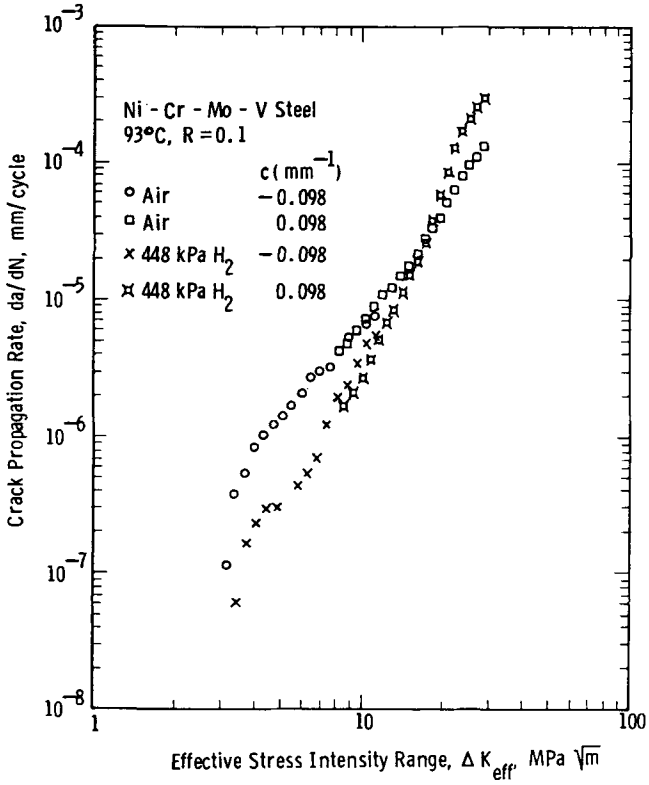

(b)

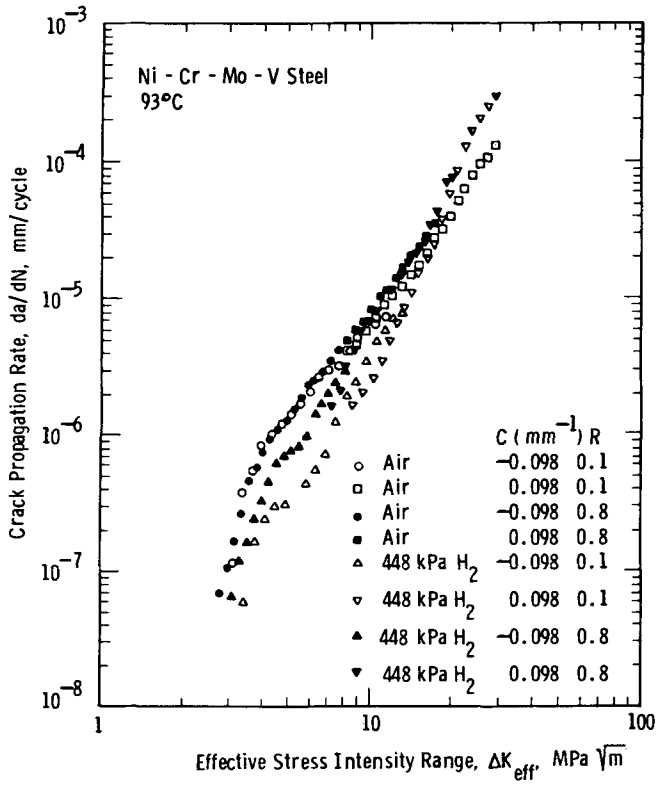

(c)

Fig. 8—(*a*) Crack closure in air and H_2. (*b*) Effect of crack closure on rates of near-threshold crack propagation in air and H_2. (*c*) Effect of crack closure on rates of near-threshold crack propagation in air and H_2 at 2 *R* ratios.

in the threshold crack growth rates in air and hydrogen environments still exists. Thus, the crack closure concept does not explain the influence of H_2 on the threshold crack propagation behavior in NiCrMoV steel at the strength level examined in this study.

Figure 8(c) shows the plot of da/dN *vs* ΔK_{eff} at $R = 0.1$ and 0.8 in air and H_2, respectively. Near the threshold, the difference in da/dN due to the influence of R ratios is greatly reduced; *e.g.*, the air environment crack growth rate data are essentially the same at $R = 0.1$ and 0.8 (Figure 8(c)). Thus, it appears that crack closure may be responsible for the effect of R values on threshold crack propagation in this steel. A similar finding was also reported in two aluminum alloys.[34]

At low ΔK values (<12 MPa$\sqrt{m}$), the crack propagation rates in argon are comparable to those in hydrogen (Figure 4). The near-threshold crack propagation rates are slower in hydrogen than in laboratory air (Figures 2(a) to 2(c)). These results suggest that the threshold fatigue crack propagation kinetics in NiCrMoV steel are controlled by the residual moisture content in the gaseous environment. As mentioned earlier, the moisture content in the hydrogen and argon environments is less than 10 ppm. This is much lower than the moisture content in laboratory air, which for 30 to 40 pct relative humidity, is equivalent to approximately 8000 to 9000 ppm. The moisture content in air is just below that found to induce capillary condensation of water in cracks grown in the Paris region for an Hll steel.[35] In the current investigation of threshold crack growth, the lower ΔK and correspondingly lower crack tip radius are likely to cause liquid water to condense at the crack tip in the air tests. Thus, the amount of water or water vapor in the

gaseous environment seems to control the observed threshold fatigue crack propagation behavior. This phenomenon is presumably due to a hydrogen embrittlement mechanism, the atomic hydrogen being generated from the H_2O-steel surface reaction. At low ΔK levels ($\lesssim$12 MPa$\sqrt{m}$), the dissociation of water appears to be favored over that of molecular hydrogen (Figures 2(a) to 2(c)). However, at higher ΔK levels ($\lesssim$12 MPa$\sqrt{m}$), the gaseous hydrogen dissociation seems to be activated (Figures 2(a), 2(b), and 4). The reason for this is not known. We suggest that this transition ΔK level corresponds to the point where adequate fresh surface is created to accommodate the production of atomic hydrogen from the gaseous dissociation reaction in addition to the H_2O-steel reaction. Below this transition level, the H_2O-steel reaction occurs preferentially and occupies all reaction sites (fresh surface).

The above interpretation is consistent with the results of Auger spectroscopy, where it was found that the oxide layer at the threshold was four times thicker in air than in hydrogen or argon (Figure 7). The thicker oxide layer in air is related to the higher moisture level, as compared to the hydrogen or argon environment.

It should be noted that in lower strength steels (less than ~600 MPa) such as 2.25Cr-1Mo steels,[16,17,19] the mentioned capillary condensation of liquid water may still be present during threshold crack growth in ambient air. However, it was reported that in air and at low R ratios (<0.5), the decreased material strength level promoted the buildup of the oxide debris at the threshold due to larger plasticity-induced crack closure (fretting oxidation) in lower strength materials.[36,37,38] Furthermore, it is known that decreasing material strength reduces the effect of hydrogen embrittlement on fatigue crack propagation behavior. Therefore, in lower strength steels at low R values, the presence of oxide-induced crack closure in air prevails over hydrogen embrittlement at the threshold levels, which results in a larger value of ΔK_{th} in air than in drier environments such as hydrogen or argon, as reported by Ritchie *et al.*[16,17,19]

B. *Fracture Morphology in Hydrogen*

Rice's formula[39] for monotonic and cyclic plastic zone sizes for a Mode I crack are as follows:

Monotonic plastic zone:

$$S_1 = \frac{\pi}{8}\left(\frac{K_{max}}{\sigma_y}\right)^2 \quad [2]$$

Cyclic plastic zone:

$$S_2 = \frac{\pi}{32}\left(\frac{\Delta K}{\sigma_y}\right)^2 \quad [3]$$

where σ_y is the yield strength. Table II lists the monotonic and cyclic plastic zone sizes for K_{max} and ΔK corresponding to the maximum proportion of intergranularity. Interestingly, the cyclic plastic zone size is on the order of the prior austenite grain size (10 to 43 μm) regardless of R ratios. However, the monotonic plastic zone size for the three values of R is approximately four to 80 times larger than the prior austenite grain size (Table II). Similar results were also found in other steels,[14,15,20,40,41] as illustrated in Table II. Therefore, in high strength low alloy steels exposed to hydrogen, the intergranular morphology of fatigue crack propagation seems to be controlled more by ΔK than K_{max}.

In Figure 1(b) in the H_2 environment, when the R ratio increases, the near-threshold fatigue crack growth rate becomes faster at a given ΔK value, as mentioned before. Nevertheless, increasing R ratios lowers the proportion of intergranularity (Figure 6). Therefore, a larger percentage of intergranular failure in hydrogen gas does not guarantee a faster crack propagation rate in NiCrMoV steel. Similarly, it was found that there was little relationship between the amount of intergranularity and the rate of crack growth for other steels[13,15,16] in air and hydrogen environments.

C. *Fatigue Crack Growth Rate Data*

The crack growth rate results in the increasing and decreasing ΔK tests with positive and negative c values, respectively, overlap each other in a certain range of da/dN *vs* ΔK; see Figures 1, 2, and 4. This overlap in results clearly indicates the uniqueness of the da/dN value at a fixed ΔK level. Such data also show that transient effects due to load shedding in the decreasing ΔK test are eliminated when loads are shed continuously and the rate of change in plastic zone size is done slowly. These factors might explain why previous results[20] on an NiCrMoV steel produced significantly higher ΔK_{th} values (7 MPa$\sqrt{m}$ *vs* 4 MPa$\sqrt{m}$) when ΔK was decreased by step loading at uncontrolled rates of plastic zone change.

For purposes of engineering applications, the crack growth rate data developed in this investigation were fitted to the equation, $da/dN = b(\Delta K)^m$. The values of b and m were computed for the near-threshold (approximately from

Table II. Values of ΔK, K_{max} and the Corresponding Plastic Zone Size at Which the Maximum Intergranular Fracture Takes Place in H_2 for Various Steels

Steel	Temperature, °C	R	ΔK, MPa $\sqrt{m}$	K_{max}, MPa $\sqrt{m}$	Monotonic Plastic Zone, μm	Cyclic Plastic Zone, μm	Grain Size, μm
Ni-Cr-Mo-V	93	0.1	11.3	12.6	115	23	10 ~ 43
Ni-Cr-Mo-V	93	0.5	11.3	22.6	369	23	10 ~ 43
Ni-Cr-Mo-V	93	0.8	11.3	56.5	2307	23	10 ~ 43
Ni-Mo-V[15]	24	0.5	10.0	19.2	331	22	7 ~ 43
Ni-Mo-V[15]	93	0.1	10.0	11.1	140	27	7 ~ 43
Ni-Mo-V[15]	93	0.5	10.0	19.2	403	27	7 ~ 43
Ni-Mo-V[15]	93	0.8	10.0	51.4	2890	27	7 ~ 43
HP-9-4-20[40]	0	0.1	23.6	26.2	112	23	20
2Ni-Cr-Mo-V[20]	24	0.1	10.0	11.1	146	30	35

5×10^{-7} to 5×10^{-8} mm per cycle) and Paris-region (approximately from 10^{-6} to 10^{-3} mm per cycle) crack growth. The values of m, b, and ΔK_{th} are listed in Tables III and IV. Note that the data on NiMoV steel are from Reference 15. In an earlier paper, Niccolls[42] has found that in the Paris-region crack propagation, there is a linear relationship between m and log b for steels and aluminum alloys, respectively. Furthermore, McCartney and Irving[43] using a dimensional analysis verified Niccolls' results. In the present study, the transition from the Paris-region to near-threshold crack growth occurs at a growth rate of approximately 10^{-6} mm per cycle. The relationship between m and log b for fatigue crack growth in NiCrMoV and NiMoV steels is shown in Figures 9(a) and 9(b) for the Paris and near-threshold regions, respectively. It is interesting to note that there is a linear relationship between m and log b in each region. The linearity between m and log b in the Paris and near-threshold regions may provide a systematic way to correlate the crack growth rate data in different environments and to validate the experimental results.

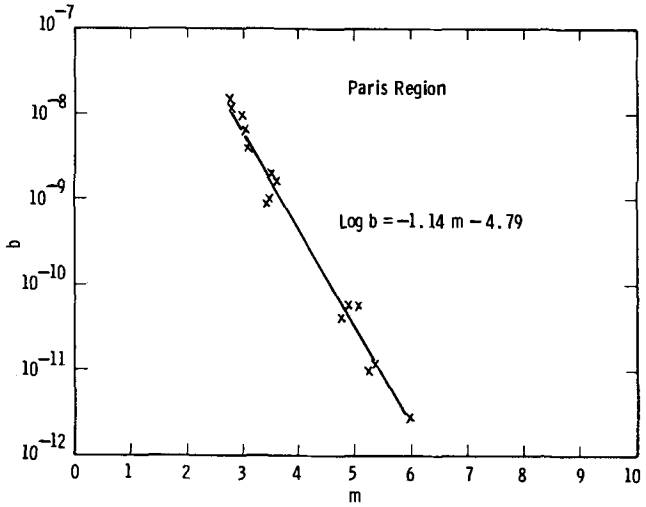

Fig. 9—(a) The relationship between m and log b in the equation, $da/dN = b(\Delta K)^m$, for NiMoV and NiCrMoV steels in Paris region. (b) The relationship between m and log b in the equation, $da/dN = b(\Delta K)^m$, for NiMoV and NiCrMoV steels in near-threshold region.

In air and argon environments, the NiMoV and NiCrMoV steels have comparable crack growth rates at $R = 0.1$, 0.5, and 0.8 (an example is shown in Figure 10(a)). However, in the hydrogen environment, the NiCrMoV steel has slightly higher near-threshold rates of crack propagation (Figures 10(b) through 10(d)). In the Paris region, the hydrogen environment crack growth rate is somewhat faster in the NiMoV steel than in the NiCrMoV steel. This trend is especially obvious at the largest value of R, 0.8, as shown in Figure 10(d). From the data by Clark and Ceschini,[22] it was found that in the Paris region, the crack growth rates in the NiMoV and NiCrMoV steels were nearly the same in air and distilled water, but in 448 kPa H_2, the fatigue crack propagated faster in the NiMoV steel. The present results are consistent with Clark and Ceschini's data and serve to emphasize the point that material and microstructural effects are accentuated when environments are present to assist fatigue crack propagation. It is worth mentioning that in Figure 6, the much larger percentage of intergranular fracture in NiCrMoV than NiMoV steels does not always correspond to a larger rate of crack growth.

VI. SUMMARY AND CONCLUSIONS

1. Near-threshold fatigue crack growth rates and ΔK_{th} values in NiCrMoV steel are the same in the hydrogen and argon environments. These rates are slower than those in laboratory air. However, as ΔK and da/dN increase, the rates in hydrogen become increasingly faster than those in argon and eventually surpass the rates in air as well. This transition in the hydrogen rates, occurring at a relatively constant $\Delta K \simeq 12$ MPa$\sqrt{\text{m}}$, is independent of R, thereby suggesting that it is controlled by cyclic deformation at the crack tip rather than by monotonic deformation or hydrostatic stress.
2. It is postulated that the above ordering of near-threshold growth rates is associated with the level of residual moisture in each environment which controls the supply of atomic hydrogen necessary for embrittlement. It appears that the dissociative adsorption of H_2O at the crack tip is favored over that of H_2 at low ΔK values. Consequently, the transition-ΔK, corresponding to an acceleration in the hydrogen crack growth rates, is believed to occur when cyclic deformations provide sufficient fresh surface to accommodate dissociative adsorption of H_2 as well as H_2O at the crack tip. Further systematic studies of the dependence of this transition on gas purity, cyclic frequency, and temperature would aid in clarifying this mechanism.
3. In both air and hydrogen environments, fatigue crack growth rates in NiCrMoV steel increase as R is increased; this effect becomes increasingly pronounced as the threshold is approached; consequently, ΔK_{th} is markedly sensitive to R. The influence of R on near-threshold growth rates is reduced considerably when data are represented in terms of the measured ΔK_{eff}, thus suggesting that crack closure significantly influences crack growth in the near-threshold regime. Nevertheless, the dependence of near-threshold growth rates on environment could not be explained in terms of crack closure concepts in this material.

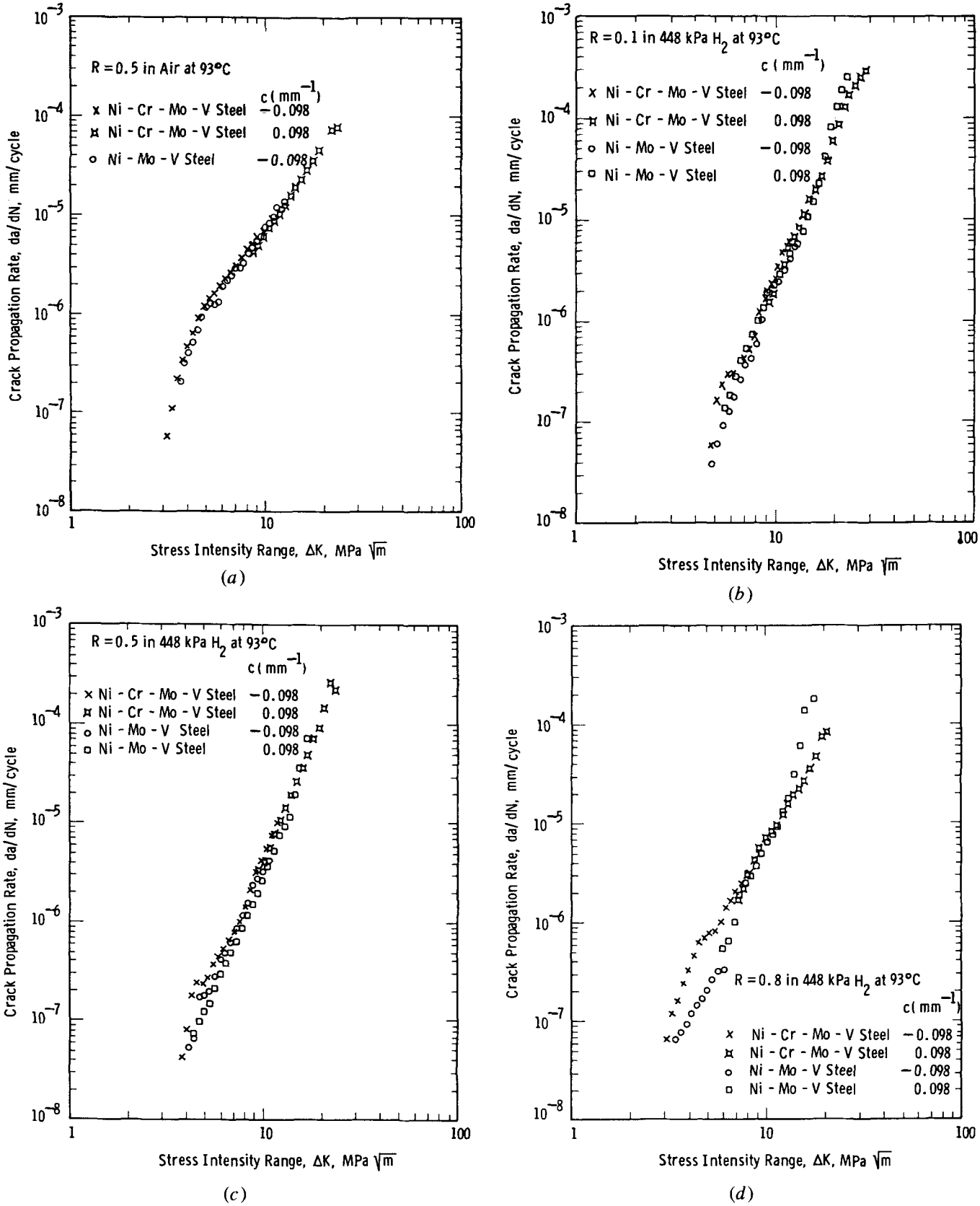

Fig. 10—(*a*) Comparison of crack growth rates in NiCrMoV and NiMoV steels in air at $R = 0.5$. (*b*) Comparison of crack growth rates in NiCrMoV and NiMoV steels in H_2 at $R = 0.1$. (*c*) Comparison of crack growth rates in NiCrMoV and NiMoV steels in H_2 at $R = 0.5$. (*d*) Comparison of crack growth rates in NiCrMoV and NiMoV steels in H_2 at $R = 0.8$.

Table III. Fatigue Crack Growth Rate Parameters for NiMoV Steel***

Environment	Temperature, °C	R	Paris Region		Near-Threshold Region		ΔK_{th} MPa$\sqrt{m}$
			b*	m*	b*	m*	
air**	24	0.5	1.57×10^{-9}	3.63	2.41×10^{-11}	5.54	4.00
air	93	0.1	3.53×10^{-9}	3.14	1.28×10^{-15}	12.0	4.54
air	93	0.5	1.17×10^{-8}	2.80	3.63×10^{-11}	6.63	3.31
air	93	0.8	9.50×10^{-9}	3.00	1.55×10^{-11}	8.18	2.92
448 kPa H_2	24	0.5	1.12×10^{-11}	5.38	1.08×10^{-12}	6.94	4.57
448 kPa H_2	93	0.1	9.63×10^{-12}	5.29	2.03×10^{-12}	6.37	5.46
448 kPa H_2	93	0.5	2.82×10^{-12}	5.97	4.59×10^{-11}	5.05	4.16
448 kPa H_2	93	0.8	5.49×10^{-11}	5.09	1.49×10^{-9}	3.06	3.94
448 kPa Ar	93	0.5	9.54×10^{-10}	3.49	2.06×10^{-10}	4.58	3.86

*$\frac{da}{dN} = b(\Delta K)^m$, units of $\frac{da}{dN}$ and ΔK are mm per cycle and MPa$\sqrt{m}$, respectively.
**From Reference 18
***From Reference 15

Table IV. Fatigue Crack Growth Rate Parameters for NiCrMoV Steel at 93 °C

Environment	R	Paris Region		Near-Threshold Region		ΔK_{th} MPa$\sqrt{m}$
		b*	m*	b*	m*	
air	0.1	4.01×10^{-9}	3.12	3.96×10^{-19}	18.3	4.20
air	0.5	6.22×10^{-9}	3.03	3.26×10^{-12}	8.72	3.27
air	0.8	1.44×10^{-8}	2.77	2.69×10^{-11}	7.72	2.90
448 kPa H_2	0.1	3.99×10^{-11}	4.77	1.14×10^{-10}	4.34	4.77
448 kPa H_2	0.5	5.50×10^{-11}	4.88	1.33×10^{-10}	4.72	4.07
448 kPa H_2	0.8	1.97×10^{-9}	3.52	1.60×10^{-10}	5.53	3.21
448 kPa Ar	0.5	8.69×10^{-10}	3.48	1.99×10^{-11}	6.07	4.07

*$\frac{da}{dN} = b(\Delta K)^m$, units of $\frac{da}{dN}$ and ΔK are mm per cycle and MPa$\sqrt{m}$, respectively.

4. The opposite trend in near-threshold fatigue crack growth rates which has been previously reported for lower strength steels,[16,17,19,20,21,38] that is, faster rates in hydrogen than in air, appears to be associated with the relatively high levels of plasticity-induced crack closure which occurs in these lower strength materials. In higher strength steels, such as that used in this study, lower levels of plasticity-induced closure preclude the buildup of significant oxides by the fretting oxidation mechanism. A systematic study of a single steel, heat treated to a range of strength levels, is needed to confirm this view.
5. The fracture morphology at the threshold was transgranular for all R values and environments studied. This morphology remained unaltered as ΔK was increased in the air and argon environments. However, in the hydrogen environment, increasing proportions of intergranular failure occurred as ΔK increased; intergranularity reached a maximum of about 30 pct, then decreased to near zero with further increases in ΔK. The maximum intergranularity occurred when the cyclic plastic zone was approximately equal to the prior austenite grain size. Although these observations are interesting, the intergranularity did not correspond to the maximum environmentally-assisted crack growth rate.
6. In the air and argon environments, fatigue crack growth rate properties in NiCrMoV and NiMoV steels were identical. However, in the hydrogen environment, the near-threshold growth rates in the NiCrMoV steel were measurably faster than those in the NiMoV steel, especially at a high R ratio of 0.8.

ACKNOWLEDGMENTS

The authors very much appreciate the critical review and encouragement from W. G. Clark, Jr., during the preparation of this manuscript. We like to thank Professor R. O. Ritchie, Professor R. P. Wei, Dr. S. Cheruvu, and Dr. L. D. Kramer for helpful discussions. Thanks are due to A. Karanovich, J. P. Yex, R. M. Slepian, M. G. Peck, and C. W. Hughes for their help in fractography. D. Detar skillfully performed the Auger analysis. The discussion with Dr. J. Schreurs on Auger results is greatly appreciated. Above all, we are very grateful to Westinghouse Electric Corporation, Technical Operations Generator Division, for financial support.

REFERENCES

1. R. J. Bucci, W. G. Clark, Jr., and P. C. Paris: in *Stress Analysis and Growth of Cracks*, ASTM STP 513, 1972, p. 177.
2. R. O. Ritchie: *International Metals Review*, 1979, vol. 20, p. 205.
3. J. Masounave and J. P. Bailon: *Scripta Met.*, 1976, vol. 10, p. 165.
4. J. Masounave and J. P. Bailon: *Proc. 2nd Int. Conf. on Mechanical Behavior of Materials*, ASM, Metals Park, OH, 1976, p. 636.
5. R. O. Ritchie: *Fracture 1977*, D. M. R. Taplin, ed., Waterloo, Ontario, University of Waterloo Press, 1977, vol. 2, p. 1325.
6. R. O. Ritchie: *Met. Sci.*, 1977, vol. 11, p. 368.
7. J. L. Robinson and C. J. Beevers: Met. Sci., 1973, vol. 7, p. 153.
8. P. E. Irving and C. J. Beevers: *Mat. Sci. Eng.*, 1974, vol. 14, p. 229.
9. G. R. Yoder, L. A. Cooley, and T. W. Crooker: *J. Eng. Matl. Tech., ASME*, 1979, vol. 101, p. 86.
10. J. McKittrick, P. K. Liaw, S. I. Kwun, and M. E. Fine: *Metall. Trans. A*, 1981, vol. 12A, p. 1535.

11. P. C. Paris, R. J. Bucci, E. T. Wessel, W. G. Clark, Jr., and T. R. Mager: in *Stress Analysis and Growth of Cracks*, ASTM STP 513, 1972, p. 141.
12. J. Petit and J. L. Maillard: *Scripta Met.*, 1980, vol. 14, p. 163.
13. P. E. Irving and A. Kurzfeld: *Met. Sci.*, 1978, vol. 12, p. 495.
14. R. J. Cooke, P. E. Irving, G. S. Booth, and C. J. Beevers: *Eng. Fract. Mech.*, 1975, vol. 7, p. 69.
15. P. K. Liaw, S. J. Hudak, Jr., and J. K. Donald: 14th National Symposium on Fracture Mechanics, ASTM STP, 1981, in press.
16. R. O. Ritchie, S. Suresh, and J. Toplosky: MIT Fatigue and Plasticity Laboratory, Report No. FPL/R/80/1030, Cambridge, MA, 1980.
17. R. O. Ritchie: Proceedings of the Intl. Conf. on Analytical and Experimental Fracture Mechanics, Rome, June 1980, G. C. Sih, ed., Sijthoff and Noordhoff, the Netherlands, p. 81.
18. T. T. Shih and J. K. Donald: *J. of Engineering Materials and Technology*, 1981, vol. 103, p. 104.
19. R. O. Ritchie, C. M. Moss, and S. Suresh: MIT Fatigue and Plasticity Laboratory, Report No. FPL/R/79/1025, Cambridge, MA, 1979.
20. A. T. Stewart: *Eng. Fract. Mech.*, 1980, vol. 13, p. 463.
21. R. O. Ritchie: MIT Fatigue and Plasticity Laboratory, Annual Report No. 1 for Department of Energy — Fossil Energy Research 12-66-79, Cambridge, MA, 1979.
22. W. G. Clark, Jr. and L. J. Ceschini: *J. of Materials for Energy Systems*, 1981, vol. 3, p. 42.
23. H. D. Greenberg, E. T. Wessel, W. G. Clark, Jr., and W. H. Pryle: Westinghouse R & D Center, Pittsburgh, PA, unpublished research, 1969.
24. W. G. Clark, Jr., Westinghouse R & D Center, Pittsburgh, PA, unpublished research, 1970.
25. Annual ASTM Standards – E647, 1980, p. 753.
26. Ashok Saxena, S. J. Hudak, Jr., J. K. Donald, and D. W. Schmidt: *J. of Testing and Evaluation*, 1978, vol. 6, p. 167.
27. Ashok Saxena and S. J. Hudak, Jr.: *Int. J. of Fract.*, 1978, vol. 14, p. 453.
28. R. J. Cooke and C. J. Beevers: *Matl. Sci. and Eng.*, 1974, vol. 13, p. 201.
29. R. J. Cooke and C. J. Beevers: *Eng. Fract. Mech.*, 1973, vol. 5, p. 1061.
30. C. S. White: SB Thesis, MIT, Cambridge, MA, May 1980.
31. M. Kikukawa, M. Jona, and K. Tanaka: Proceedings of the Second International Conf. on Mechanical Behavior of Materials, N. Promisel and V. Weiss, eds., Boston, MA, ASM, Metals Park, OH, 1976, p. 716.
32. S. Purushothaman and J. K. Tien: Fifth Conference on the Strength of Metals and Alloys, Proc. ICSMA5 Conf., Pergamon Press, New York, NY, 1979, vol. 2, p. 1267.
33. A. J. McEvily: *Metal Science*, 1977, vol. 11, p. 274.
34. J. A. Vazquez, A. Morrone, and H. Ernst: *Eng. Fract. Mech.*, 1979, vol. 12, p. 231.
35. H. H. Johnson and A. M. Willner: *Applied Materials Research*, 1965, vol. 4, p. 34.
36. J. Toplosky and R. O. Ritchie: *Scripta Met.*, 1981, vol. 15, p. 905.
37. P. K. Liaw, T. R. Leax, R. S. Williams, and M. G. Peck: *Acta Met.*, in press.
38. R. O. Ritchie, S. Suresh, and P. K. Liaw: Proceedings of the 1st Int. Conference on Ultrasonic Fatigue and Corrosion Fatigue, J. M. Wells, *et al*, eds., *TMS-AIME*, Warrendale, PA, 1982, in press.
39. J. R. Rice: in *Fatigue Crack Propagation*, ASTM STP 415, 1967, p. 247.
40. J. D. Frandsen and H. L. Marcus: *Scripta Met.*, 1975, vol. 9, p. 1089.
41. G. R. Yoder, L. A. Cooley, and T. W. Crooker: 14th National Symposium on Fracture Mechanics, ASTM STP, 1981, in press.
42. E. H. Niccolls: *Scripta Met.*, 1976, vol. 10, p. 295.
43. L. N. McCartney and P. E. Irving: *Scripta Met.*, 1977, vol. 11, p. 181.